Supporting Information

for

Highly efficient bacterial removal and disinfection by magnetic barium phosphate nanoflakes with embedded iron oxide nanoparticles

Junyi Song [a, b, ‡], *Fan Zhang* [c, d, ‡, *], *Yuxiong Huang* [d], *Arturo A. Keller* [d], *Xiaoxiu Tang* [c], *Wanning Zhang* [e], *Weibin Jia* [f], *Jerome Santos* [b]

a College of Science, National University of Defense Technology, Changsha 410073, China

b Institute for Collaborative Biotechnologies, University of California, Santa Barbara, CA 93106, USA.

c College of Sciences, Nanjing Agricultural University, Nanjing 210095, PR China.

d Bren School of Environmental Science and Management, University of California, Santa Barbara, CA 93106, USA.

e School of Chemistry and Chemical Engineering, Shanghai Jiao Tong University, Shanghai 200240, PR China.

f College of Life Sciences, Nanjing Agricultural University, Nanjing 210095, PR China.

‡These authors contributed equally.

* Corresponding Author (Fan Zhang): Tel & Fax: 86-25-84396098; E-mail: zhangfan0128@njau.edu.cn

This supporting information is 15 pages long and contains 15 figures (Figures S1-S15) and 1 table (Tables S1).

S1. Characterization experiment

S1.1. Optical microscope

Gram staining method generally involves in four steps, including initial dyeing, mordant dyeing, decolorization and redyeing. The specific method is:

1- Add one drop suspension of cells to a clean glass slide and spread the drop with a loop over the surface of the slide. Allow to air-dry.

2- After drying, the glass slides are fixed by the flame.

3- Stain sample with ammonium oxalate crystal violet drops for 1 min, then rinse with water.

4- Stain sample with iodine dye for 1 min, then rinse with water.

5- Decolorized the slide with 95% ethanol for 20-30s. Slide should not be purple after this.

6- Immediately redye with sarranine for 3-5 min. Then rinse with water.

7- The stained glass slides were examined with an optical microscope.

S1.2. Fluorescent-based cell live/dead test

The bacteria death analysis was also ascertained by fluorescent-based cell live/dead test. A single colony was transferred into a tube with 5 mL LB, incubated with 37 °C for 16 h, at 220 rpm. At this point, collected bacteria at low speed centrifuge (4000 × G) and rinsed cells with ddH_2O, repeat for three times. For the last time, resuspend bacterial cells with 200 ml ddH_2O (40 folds as initial LB volume), to obtain a desired intensity about (5×10^8 CFU/mL). 200 ml of this bacterial solution was used to mix with the as-prepared materials in this work, incubating by a rotary shaker at 180 rpm for 30

min. Then fluorescent stains were added into bacteria-material mixture, incubated for 15 min before microscopy observation (Leica SP8 Resonant Scanning Confocal). Two stains contains in the LIVE/DEAD®BacLightTM Bacterial Viability Kit: SYTO9 is a cell-permeable green-fluorescent stain, which labels both live and dead bacteria; whereas PI is a cell-impermeable red-fluorescent stain that only labeled cells with a compromised membrane, which includes cells to be dead or dying.

To test toxicity and interaction of the cations in FBP and FNPs (Fe^{3+}, Fe^{2+}, Ba^{2+}) to *E. coli*, different solutions containing the similar concentration in materials was obtained by solving $FeCl_3 \cdot 6H_2O$, $FeCl_2 \cdot 4H_2O$, or $BaCl_2 \cdot 2H_2O$ into nanopure water according to the material's chemical stoichiometry, atomic ratio in EDS results, and material dosage of 0.1 g/50 mL in the removal experiment. To add 0.1285 g $FeCl_2 \cdot 4H_2O$, 0.1746 g $FeCl_3 \cdot 6H_2O$, and 0.061 g $BaCl_2 \cdot 2H_2O$ into 50 mL *E. coli* suspension (C_0=5×10^8 CFU/mL), respectively, can obtain solution sample A, B, and C. According to the maximum cation concentration from 0.1g FBP in the water, 0.061g $BaCl_2 \cdot 2H_2O$, 0.0093 g $FeCl_2 \cdot 4H_2O$ and 0.025 g $FeCl_3 \cdot 6H_2O$ is mixed into 50 mL *E. coli* suspension (C_0=5×10^8 CFU/mL) to obtain sample D. Likewise, sample E is obtained by solving 0.043g $FeCl_2 \cdot 4H_2O$ and 0.1164 g $FeCl_3 \cdot 6H_2O$ into 50 mL *E. coli* suspension (C_0=5×10^8 CFU/mL) to stimulate the maximum cation concentration from 0.1 g Fe_3O_4 in the water. All these samples were analyzed by fluorescence detection. In order to eliminate the disturbance of these cation to the red signal in fluorescence detection, we re-measured those samples after three days (stored in room temperature), and treated them with 60 ^{o}C for 5 min. By doing this, all bacterial should be dead or at least in an

injured state. Red signal from PI is successfully observed, indicating that those metal ions will not disturb the signals (not shown).

S1.3. SEM of *E. coli* with material

For the SEM observations of bacterial samples, treated bacterial samples with material were separated from the solution by a magnetic. Then the wet samples were dropped onto clean electron microscopic sample stage, fixed with a drop of 3% glutaraldehyde, stored at room temperature with a semi-closed glass cover for 3 h, analyzed by SEM.

S1.4. Dilution plate count method

Dilution plate count is based on the formation of single colonies by an initial single cell. The detailed process in this work is as follows：After *E. coli* capture (C_0=5×10^8 CFU/mL, pH=6, 25 °C, 30 min, material dosage of 2.0 mg/mL), the materials (FBP or FNP) were reclaimed by a magnet and then washed by 50 mL ddH_2O. The solution was then diluted 10^3 and 10^4 times with ddH_2O. Viable bacteria were determined by standard plate count method. The plates were incubated at 37 ^{o}C for 24 h. The number of colonies was enumerated through visual inspection.

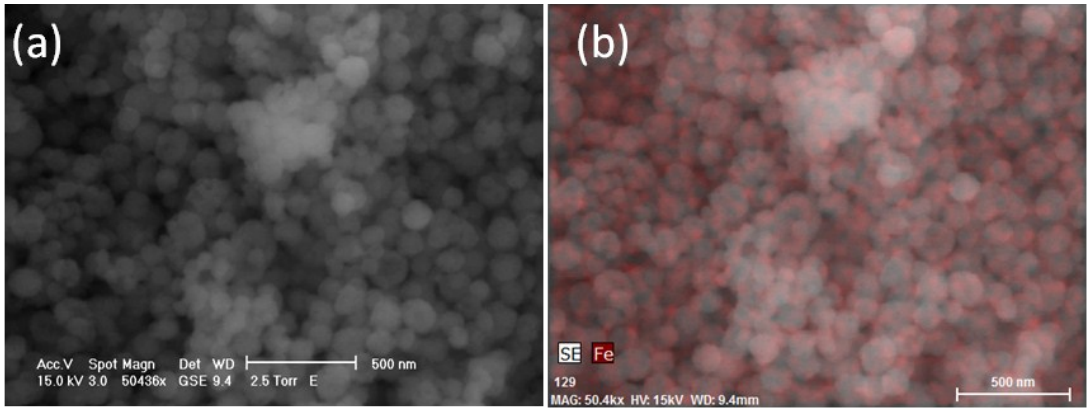

Figure S1. SEM picture of Fe_3O_4 nanoparticle.

S2. Effect of temperature

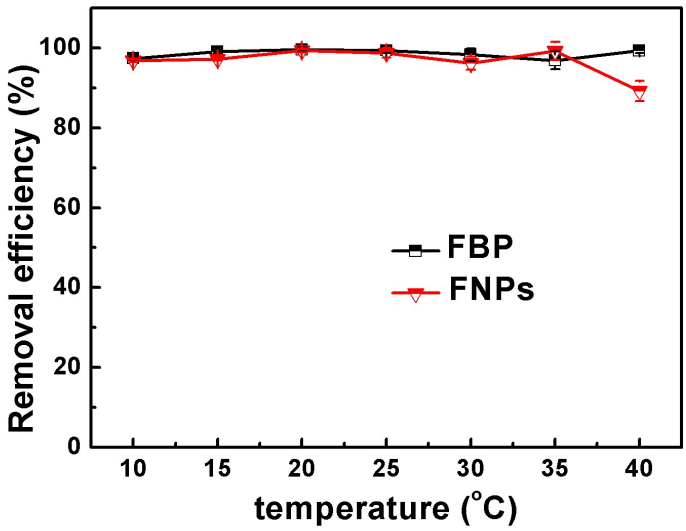

Figure S2. Removal efficiency of *E. coli* (C_0=5×10^8 CFU/mL, pH 6, 30 min) by 2.0 mg/mL of FBP and FNPs at different temperature ranging from 10 to 40 °C.

As shown in Figure S2, the removal percent of *E. coli* by FBP and FNPs showed little change in the investigated temperature range, implying the removal process is not thermodynamically controlled. The high adaptability to different temperature shows their high application potential in actual treatment.

S3. Effect of dosage

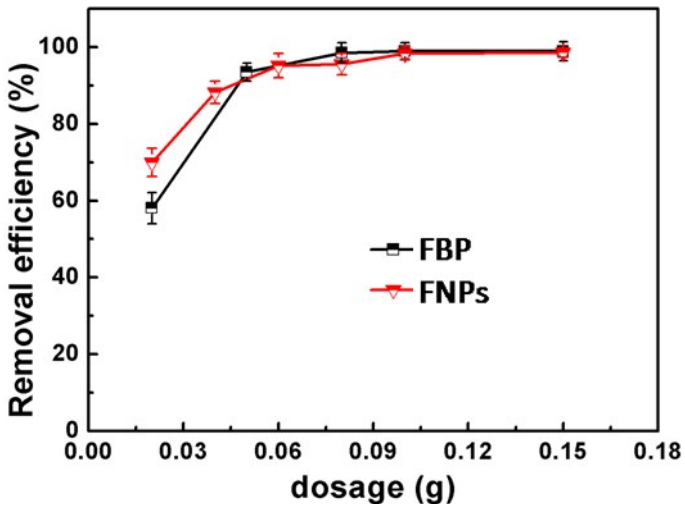

Figure S3. Removal efficiency of *E. coli* (C_0=5×10^8 CFU/mL, 50 mL, 25 °C, pH 6, 30 min) by different dosage of FBP and FNPs.

Removal efficiency of *E. coli* by FBP and FNPs as a function of dosage is illustrated in Figure S3. Removal rates are initially rapidly improved with the added dosage from 0.02 g to 0.08 g due to the increased accessible sites for bacterial capture. Above 0.08 g, there is minimal increase in removal rate. With a dosage of 0.10 g, the removal percentage of *E. coli* by FBP (99%) approaches that of FNPs after 30 min. In the following experiments, the dosage of 0.10 g was considered to be suitable for treating 50 mL of *E. coli* solutions (C_0=5×10^8 CFU/mL) by these magnetic phosphate composites within 30 min.

S4. Effect of initial *E. coli* concentration

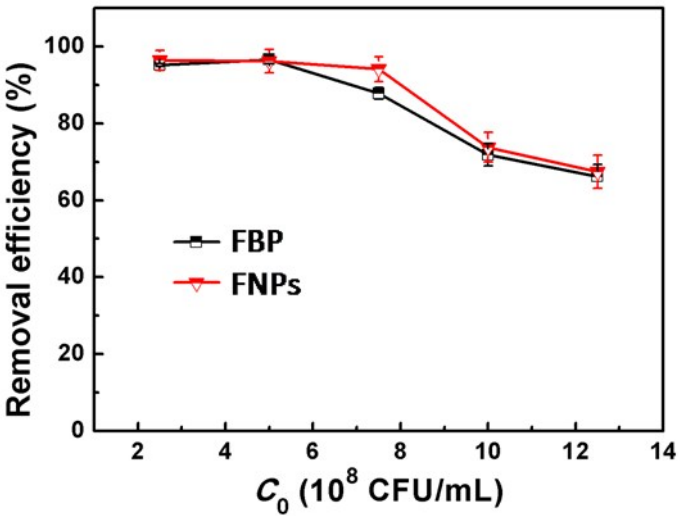

Figure S4. Removal efficiency of *E. coli* suspension with different initial concentration (25 °C, pH 6, 30 min) by 2.0 mg/mL of FBP and FNPs.

As shown in Figure S4, the initial concentration of *E. coli* suspension has obvious effect on the removal efficiency by the as-prepared FBP and FNPs. The maximum percentage was found to be 97% for both FBP and FNPs at the initial concentration of 5×10^8 CFU/mL. The slightly improved removal ratios from 2.5×10^8 CFU/mL to 5×10^8 CFU/mL can be ascribed to the increased osmotic pressure, which is helpful for the

reach of bacteria to the material's surface. Then the regularly decreased removal ratio by materials can be attributed to the saturated surface sites for bacterial capture. Comparisons of removal capacity by different magnetic materials in this work and some other recent reports are listed in Table S1. The higher removal capacity in this work confirms FBP as an efficient, competent, and promising material for removal of *E. coli* from solution.

Table S1. Comparisons of removal capacity for *E. coli* by per mg material (CFU/mg) in this work with other recent reports.

Material	Removal capacity (CFU/mg)	Reference
Fe_3O_4-SiO_2-NH_2 NPs	32.7	1
Fe_3O_4-ZnO nanocomposite	1.05×10^7	2
Magnetic graphene composite	3.72×10^6	3
Amino acid modified magnetic NPs	1.82×10^7	4
Bacteriophage-based nanoprobes	5.1×10^6	5
Anti-fimbrial modified magnetic reduced grapheme oxide nanoheaters	1.24×10^6	6
Ag-$CoFe_2O_4$-GO nanocomposite	1.98×10^6	7
Magnetic chitosan-graphene oxide composite	4.95×10^6	8
Fe_3O_4@CTAB	2.97×10^7	9
Immunomagnetic particles	900	10
FBP nanoflake	2.43×10^8	This work

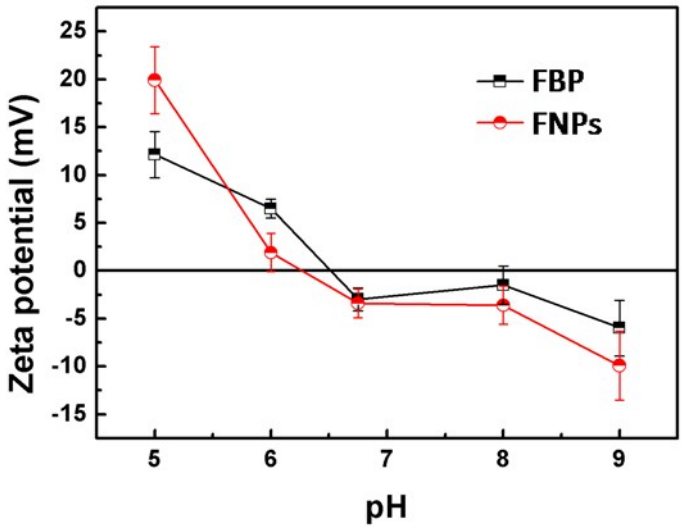

Figure S5. Zeta potentials of FBP and FNPs at different pH.

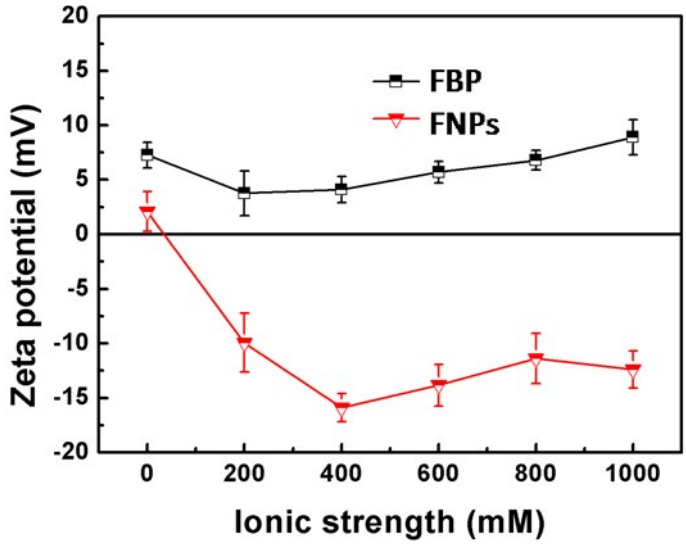

Figure S6. Zeta potentials of FBP and FNPs mixed with different concentration of NaCl.

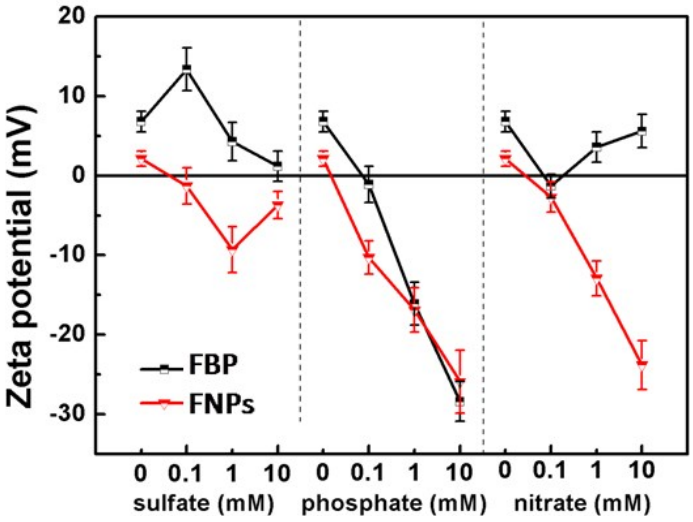

Figure S7. Zeta potentials of FBP and FNPs mixed with different co-exiting anions.

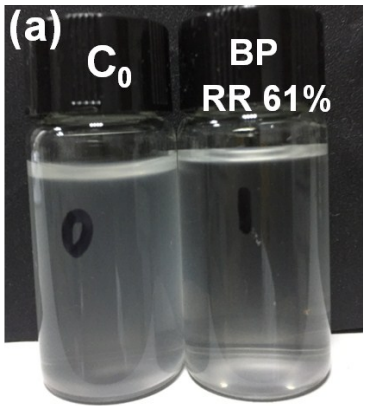

Figure S8. The removal ratio (RR) of *E. coli* from solution by rare barium phosphate (BP) nanoflake (C_0=5×10^8 CFU/mL, 25 °C, pH 6, 10 min).

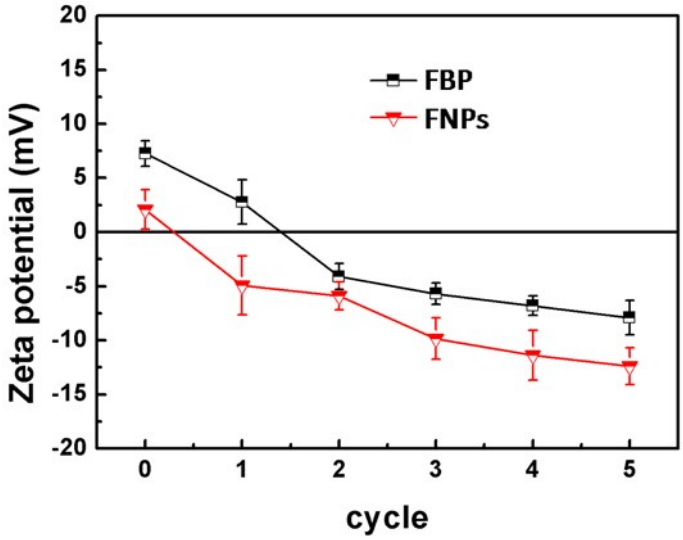

Figure S9. Zeta potentials of FBP and FNPs mixed at different cycle.

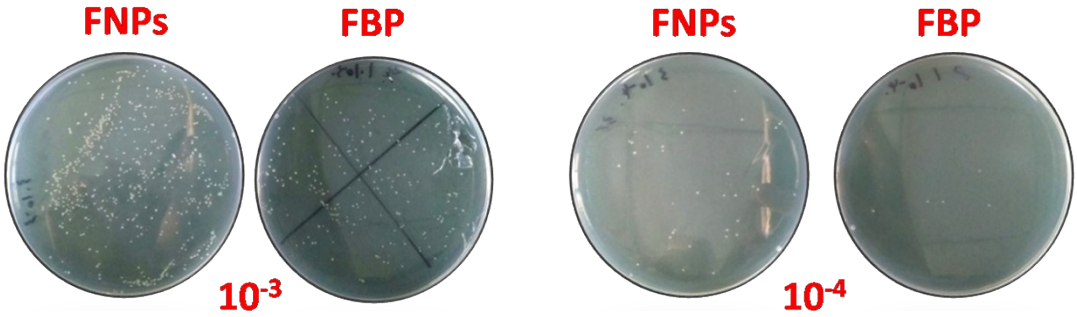

Figure S10. Dilution plating procedure results with a dilution ratio of (a) 10^{-3} and (b) 10^{-4} from the reclaimed FBP and FNPs after bacterial removal (C_0=5×10^8 CFU/mL, 25 °C, pH 6, 30 min).

S5. Effect of interaction time

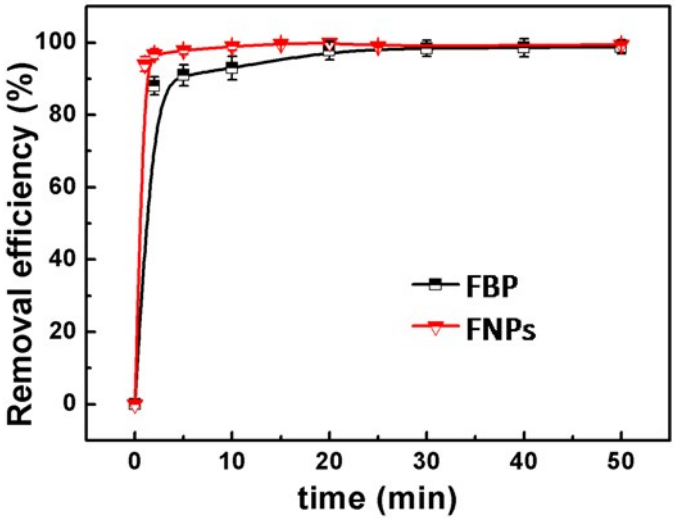

Figure S11. Removal efficiency of *E. coli* (C_0=5×10^8 CFU/mL, 25 °C, pH 6) by 2.0 mg/mL of FBP and FNPs with different interaction time.

The influence of treatment time in removal efficiency of *E. coli* by FBP and FNPs is depicted in Figure S11. It was observed that the removal effects increased gradually with the extension of reaction time. The removal efficiency of FBP is a little lower than that of FNPs during 0-25 min and then approaches the removal efficiency of FNPs after 30 min (97%). *E. coli* contaminated water changes from milky to clear after applying FBP (Figure S12). As stated above, the binding of bacteria and FBP may be formed by charge neutralization at pH 6. FBP possess a plane structure and bigger size than *E. coli* cells which may be helpful for bacterial adhesion onto FBP's surface.

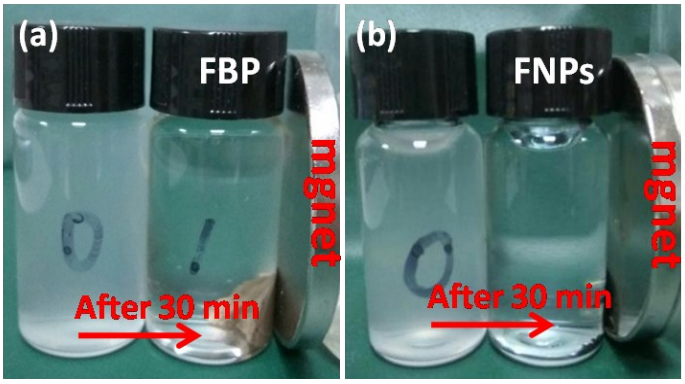

Figure S12. Removal efficiency of *E. coli* and magnetic separation by a magnet after treatment by (a) FBP and (b) FNPs (C_0=5×10^8 CFU/mL, 25 °C, pH 6, 2.0 mg/mL, 10 min).

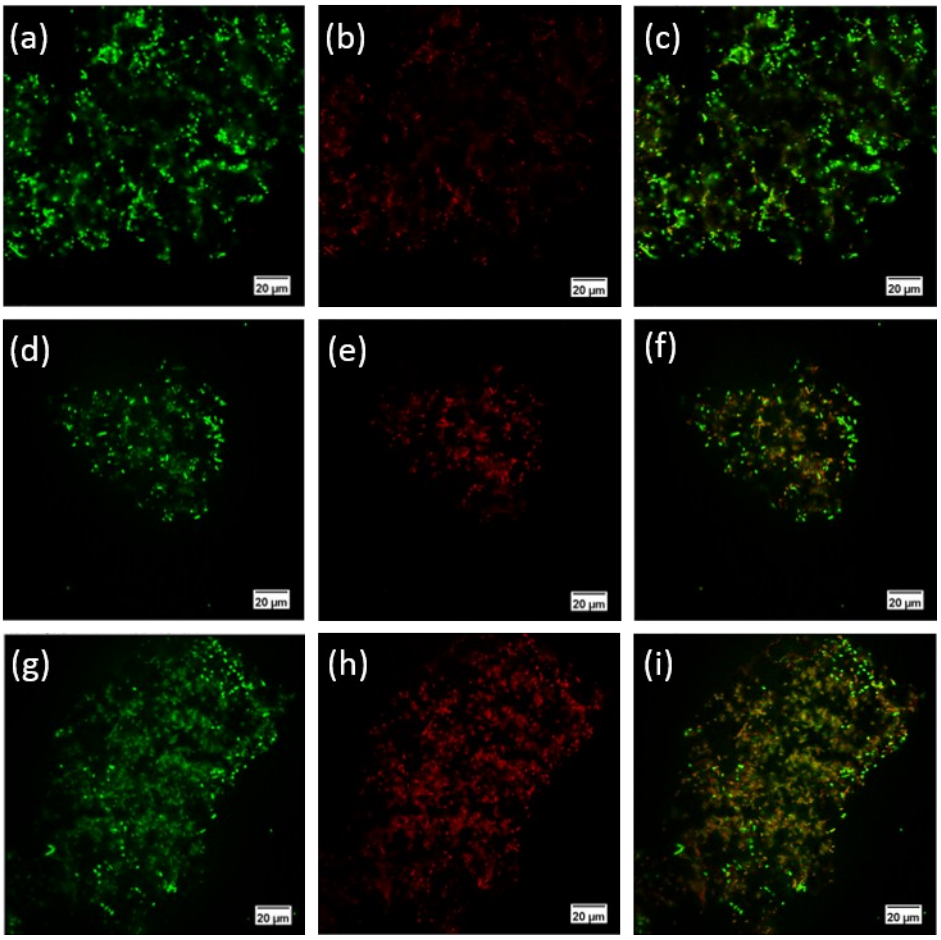

Figure S13. Confocal fluorescent images of live and dead bacterial cells treated with FBP under shaking after (a-c) 5 min, (d-f) 10 min, and (g-i) 30 min, stained with SYTO9 (green) and PI (red). (c, f, i) Overlying images of *E. coli* stained with SYTO9 (live and dead) and PI (dead).

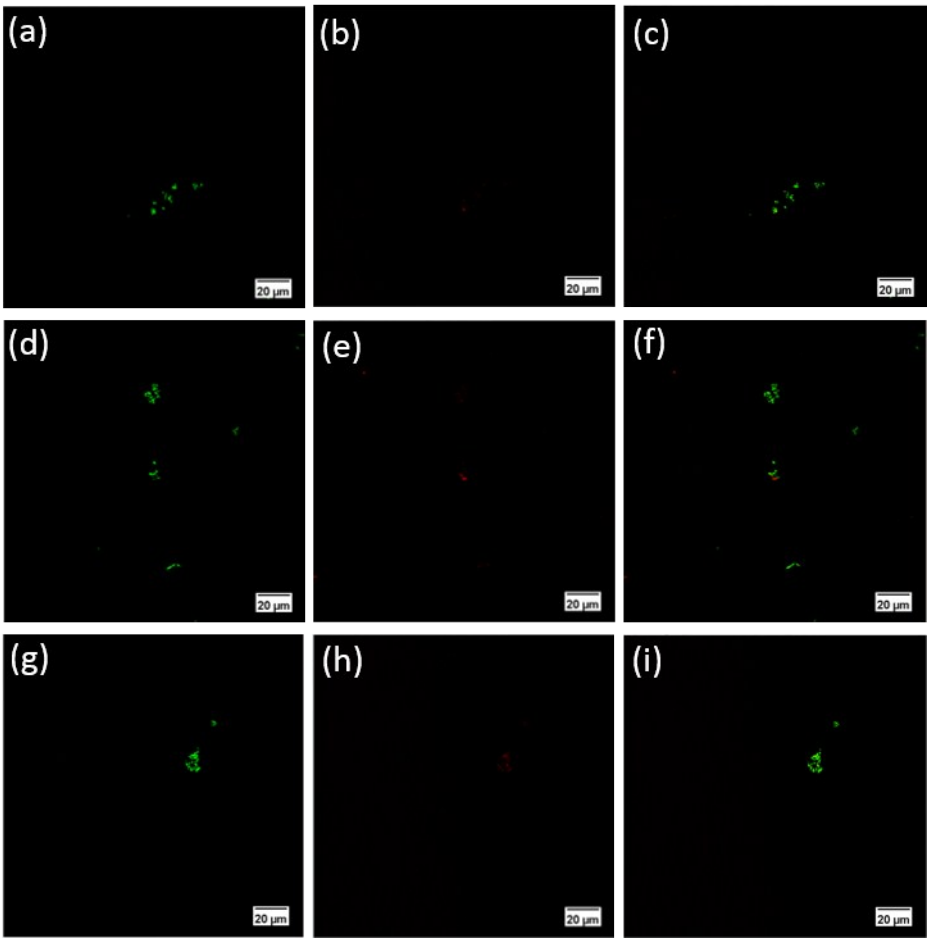

Figure S14. Confocal fluorescent images of live and dead bacterial cells treated with FNPs under shaking after (a-c) 5 min, (d-f) 15 min, and (g-i) 30 min, stained with SYTO9 (green) and PI (red). (c, f, i) Overlying images of *E. coli* stained with SYTO9 (live and dead) and PI (dead).

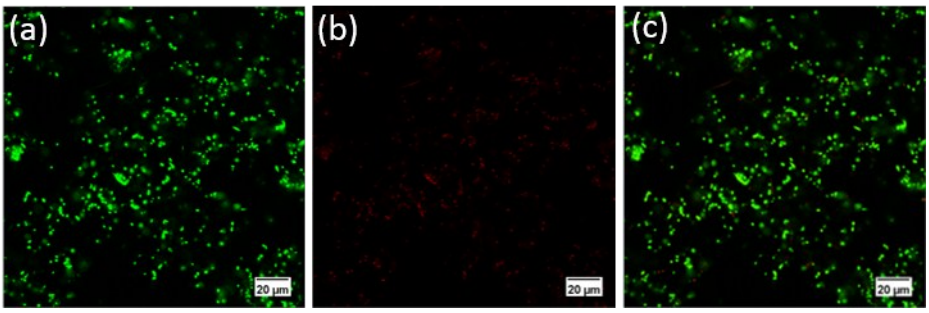

Figure S15. Confocal fluorescent images of live and dead *E. coli* cells treated with FBP without stirring, stained with SYTO9 (green) and PI (red). (c) Overlying images of *E. coli* stained with SYTO9 (live and dead) and PI (dead).

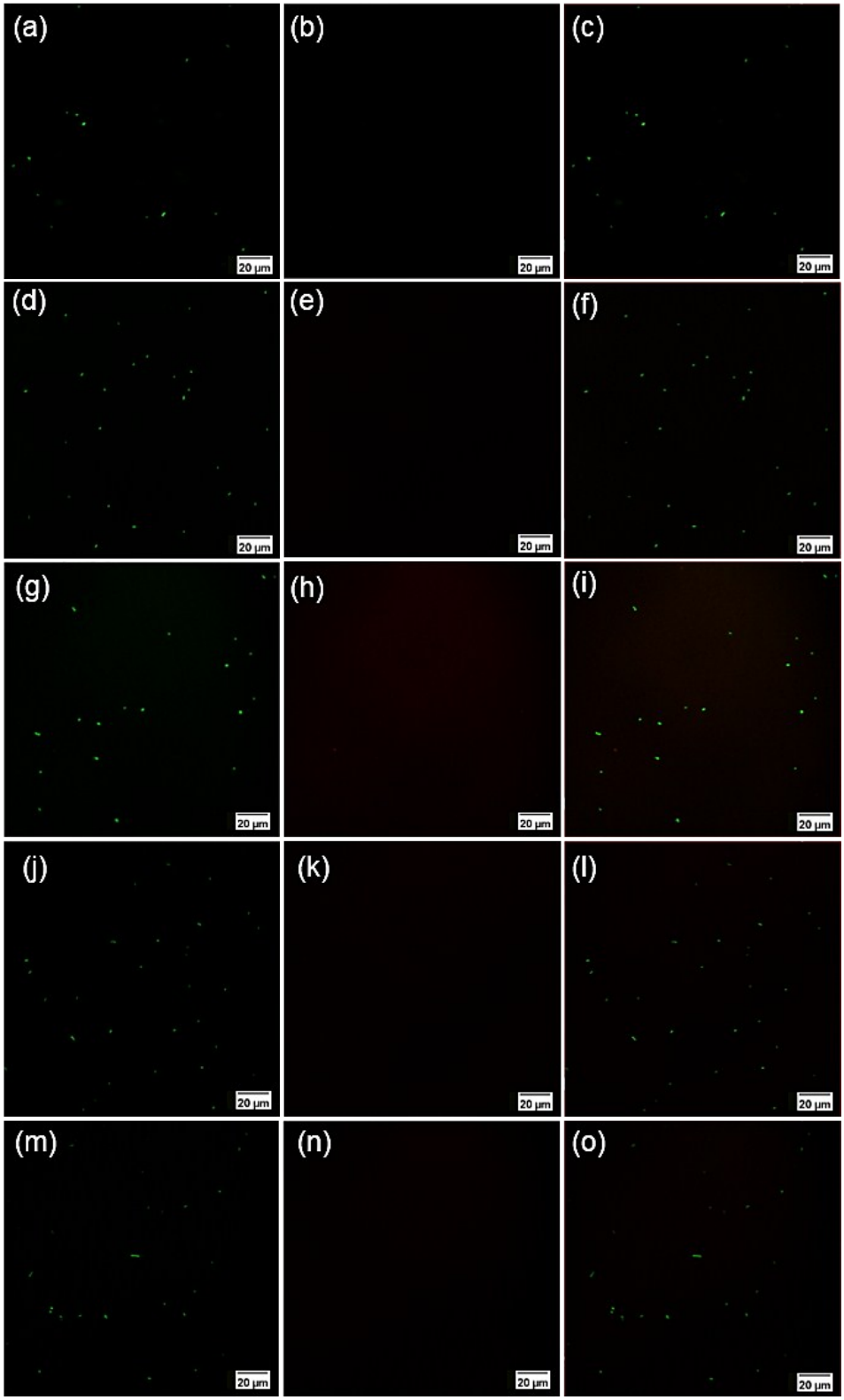

Figure S16. Confocal fluorescent images of live and dead *E. coli* cells treated in solutions containing Fe^{2+} (a−c), Fe^{3+} (d−f), Ba^{2+} (g-i), Ba^{2+}+Fe^{2+}+Fe^{3+} (j−l), and Fe^{2+}+Fe^{3+} (m−o) stained with SYTO9 (green) and PI (red). (c, f, i, l, o) Overlying images of *E. coli* stained with SYTO9 (live and dead) and PI (dead).

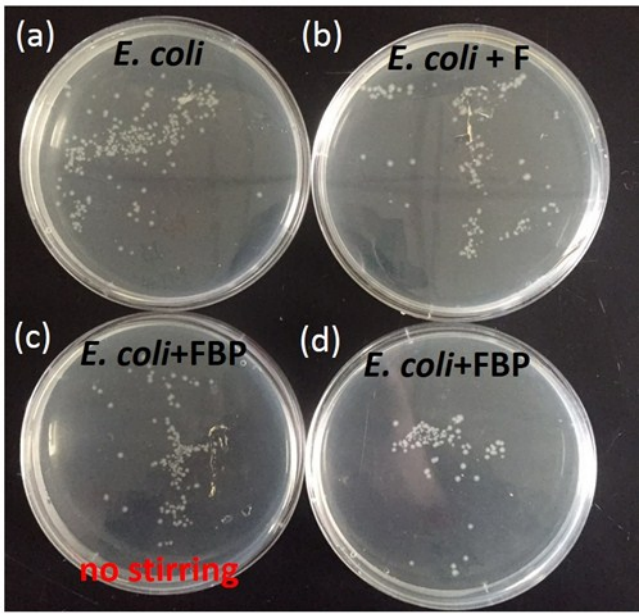

Figure S17. Bacterial cell proliferation assays of (a) pure *E. coli* and *E. coli* treated by (b) FNPs under stirring, (c) FBP without stirring, (d) FBP under stirring. In all cases, treatment condition: C_0=5×10^8 CFU/mL, 25 °C, pH 6, 30 min; sample procedure: without dying with bacterial viability kit, 5 μl 1000-folds diluted samples were coated to LB plates at 37 °C for16 h.

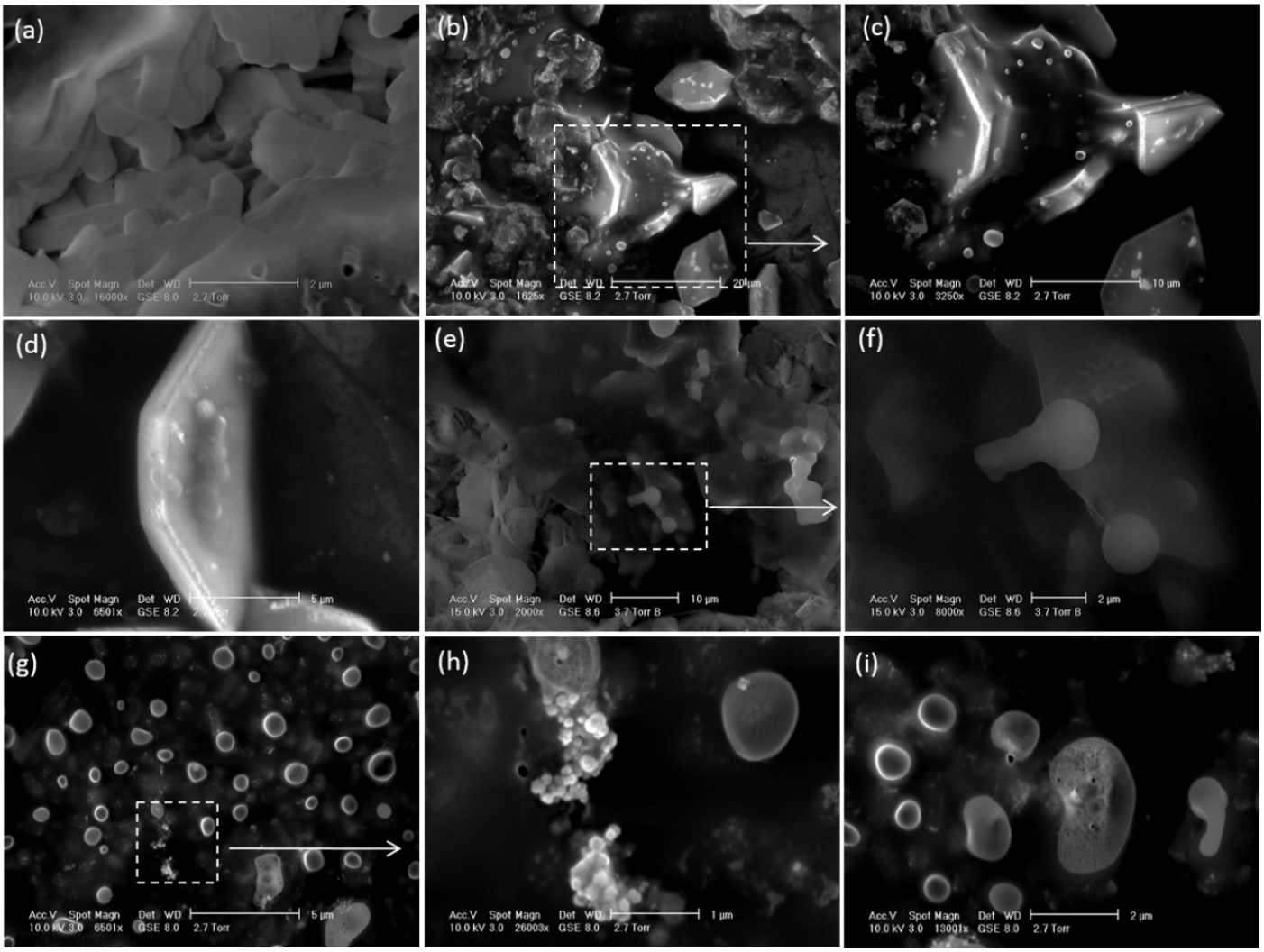

189

190 **Figure S18.** SEM images of (a) *E. coli* (obtained by centrifugation), (b-f) *E. coli* treated
191 with FBP, and (g-i) *E. coli* treated with FNPs after magnetic separation (C_0=5×10^8
192 CFU/mL, 25 °C, pH 6, material dosage 2.0 mg/mL, 30 min).

References

1. S. Zhan, Y. Yang, Z. Shen, J. Shan, Y. Li, S. Yang and D. Zhu, Efficient removal of pathogenic bacteria and viruses by multifunctional amine-modified magnetic nanoparticles, *Journal of hazardous materials*, 2014, **274**, 115-123.
2. S. Singh, K. Barick and D. Bahadur, Inactivation of bacterial pathogens under magnetic hyperthermia using Fe 3 O 4–ZnO nanocomposite, *Powder Technology*, 2015, **269**, 513-519.
3. S. Zhan, D. Zhu, S. Ma, W. Yu, Y. Jia, Y. Li, H. Yu and Z. Shen, Highly efficient removal of pathogenic bacteria with magnetic graphene composite, *ACS applied materials & interfaces*, 2015, **7**, 4290-4298.
4. Y. Jin, F. Liu, C. Shan, M. Tong and Y. Hou, Efficient bacterial capture with amino acid modified magnetic nanoparticles, *Water research*, 2014, **50**, 124-134.
5. J. Chen, B. Duncan, Z. Wang, L.-S. Wang, V. M. Rotello and S. R. Nugen, Bacteriophage-based nanoprobes for rapid bacteria separation, *Nanoscale*, 2015, **7**, 16230-16236.
6. F. Halouane, R. Jijie, D. Meziane, C. Li, S. K. Singh, J. Bouckaert, J. Jurazek, S. Kurungot, A. Barras and M. Li, Selective isolation and eradication of E. coli associated with urinary tract infections using anti-fimbrial modified magnetic reduced graphene oxide nanoheaters, *Journal of Materials Chemistry B*, 2017, **5**, 8133-8142.
7. S. Ma, S. Zhan, Y. Jia and Q. Zhou, Highly efficient antibacterial and Pb (II) removal effects of Ag-CoFe2O4-GO nanocomposite, *ACS applied materials & interfaces*, 2015, **7**, 10576-10586.
8. Y. Jiang, J.-L. Gong, G.-M. Zeng, X.-M. Ou, Y.-N. Chang, C.-H. Deng, J. Zhang, H.-Y. Liu and S.-Y. Huang, Magnetic chitosan–graphene oxide composite for anti-microbial and dye removal applications, *International journal of biological macromolecules*, 2016, **82**, 702-710.
9. Y. Jin, J. Deng, J. Liang, C. Shan and M. Tong, Efficient bacteria capture and inactivation by cetyltrimethylammonium bromide modified magnetic nanoparticles, *Colloids and Surfaces B: Biointerfaces*, 2015, **136**, 659-665.
10. J. Lin, M. Li, Y. Li and Q. Chen, A high gradient and strength bioseparator with nano-sized immunomagnetic particles for specific separation and efficient concentration of E. coli O157: H7, *Journal of Magnetism and Magnetic Materials*, 2015, **378**, 206-213.